Cerebello-thalamic activity drives an abnormal motor network into dystonic tremor

Freek Nieuwhof, Ivan Toni, Michiel F Dirkx, Cecile Gallea, Marie Vidailhet, Arthur W. G. Buijink, Anne-Fleur van Rootselaar, Bart P. C. van de Warrenburg, Rick C Helmich

NeuroImage: Clinical 33 (2022) 102919

Contents lists available at ScienceDirect

NeuroImage: Clinical

journal homepage: www.elsevier.com/locate/ynicl

Cerebello-thalamic activity drives an abnormal motor network into dystonic tremor

Freek Nieuwhof [a], Ivan Toni [a], Michiel F. Dirkx [b], Cecile Gallea [c], Marie Vidailhet [d], Arthur W. G. Buijink [e], Anne-Fleur van Rootselaar [e], Bart P.C. van de Warrenburg [b], Rick C. Helmich [a,b,*]

[a] Centre for Cognitive Neuroimaging, Donders Institute for Brain, Cognition and Behaviour, Radboud University, 6500 HB Nijmegen, the Netherlands
[b] Department of Neurology, Centre of Expertise for Parkinson & Movement Disorders, Donders Institute for Brain, Cognition and Behaviour, Radboud University Medical Centre, 6500 HB Nijmegen, the Netherlands
[c] MOV'IT Section (Movement Investigations and Therapeutics), Paris Brain Institute (CNRS/INSERM UMR 7225/1127), Sorbonne Université, 75013 Paris, France
[d] Institut du Cerveau et de la Moelle épinière (ICM) UMR 1127, Hôpital de la Pitié-Salpétrière, Department of Neurology, AP-HP, Sorbonne Université, 75013 Paris, France
[e] Department of Neurology, Amsterdam University Medical Centers, 1105 AZ Amsterdam Neuroscience, University of Amsterdam, Amsterdam, the Netherlands

ARTICLE INFO

Keywords:
Dystonia
Tremor
functional MRI
Dystonic tremor

ABSTRACT

Dystonic tremor syndromes are highly burdensome and treatment is often inadequate. This is partly due to poor understanding of the underlying pathophysiology. Several lines of research suggest involvement of the cerebello-thalamo-cortical circuit and the basal ganglia in dystonic tremor syndromes, but their role is unclear. Here we aimed to investigate the contribution of the cerebello-thalamo-cortical circuit and the basal ganglia to the pathophysiology of dystonic tremor syndrome, by directly linking tremor fluctuations to cerebral activity during scanning.

In 27 patients with dystonic tremor syndrome (dystonic tremor: n = 23; tremor associated with dystonia: n = 4), we used concurrent accelerometery and functional MRI during a posture holding task that evoked tremor, alternated with rest. Using multiple regression analyses, we separated tremor-related activity from brain activity related to (voluntary) posture holding. Using dynamic causal modelling, we tested for altered effective connectivity between tremor-related brain regions as a function of tremor amplitude fluctuations. Finally, we compared grey matter volume between patients (n = 27) and matched controls (n = 27).

We found tremor-related activity in sensorimotor regions of the bilateral cerebellum, contralateral posterior and anterior ventral lateral nuclei of the thalamus (VLp and VLa), contralateral primary motor cortex (hand area), contralateral pallidum, and the bilateral frontal cortex (laterality with respect to the tremor). Grey matter volume was increased in patients compared to controls in the portion of contralateral thalamus also showing tremor-related activity, as well as in bilateral medial and left lateral primary motor cortex, where no tremor-related activity was present. Effective connectivity analyses showed that inter-regional coupling in the cerebello-thalamic pathway, as well as the thalamic self-connection, were strengthened as a function of increasing tremor power.

These findings indicate that the pathophysiology of dystonic tremor syndromes involves functional and structural changes in the cerebello-thalamo-cortical circuit and pallidum. Deficient input from the cerebellum towards the thalamo-cortical circuit, together with hypertrophy of the thalamus, may play a key role in the generation of dystonic tremor syndrome.

Abbreviations: BFM, Burke-Fahn-Marsden dystonia rating scale; DBS, deep brain stimulation; DCM, dynamic causal modelling; GMV, grey matter volume; GPi, Internal globus pallidum; ICV, Intracranial volume; TRS, Tremor rating scale; VBM, Voxel based morphometry; VIM, ventral intermediate nucleus; VOp, ventro-oralis posterior nucleus.

* Corresponding author at: Department of Neurology, Donders Institute for Brain, Cognition and Behaviour, Radboud University Medical Centre, PO Box 9101, 6500 HB Nijmegen, the Netherlands.

E-mail address: Rick.Helmich@radboudumc.nl (R.C. Helmich).

https://doi.org/10.1016/j.nicl.2021.102919
Received 27 October 2021; Received in revised form 10 December 2021; Accepted 15 December 2021
Available online 16 December 2021

1. Introduction

Postural tremor is a highly burdensome symptom that is present in 17–55% of patients with dystonia (Defazio et al., 2013; Erro et al., 2014; Shaikh et al., 2020). Tremor is defined as an involuntary, rhythmic, oscillatory movement of a body part (Bhatia et al., 2018). Two types of dystonic tremor syndrome are distinguished: dystonic tremor, defined as tremor in a body part affected by dystonia, and tremor associated with dystonia, defined as tremor in a non-dystonic body part. Clinically, dystonic tremor syndrome typically involves an action tremor (but it may also occur during rest), tremor occurrence can be position or task-specific, and the tremor often has an irregular aspect (Wardt et al., 2020). Current treatments, such as deep brain stimulation (DBS), pharmacological interventions, or botulinum toxin, often have unsatisfactory results (Fasano et al., 2014; Cury et al., 2017). Precise knowledge about the underlying pathophysiology of dystonic tremor syndromes is lacking, preventing mechanism-based treatments. However, to date, only few studies have investigated the pathophysiology of dystonic tremor syndromes, and no studies focused on tremor-related brain activity.

Dystonic tremor syndromes may partly share pathophysiological mechanisms with dystonia itself, or with tremor syndromes that are phenotypically similar, such as essential tremor (van der Stouwe et al., 2020). One possibility is that the pathophysiology of dystonic tremor syndrome involves the cerebello-thalamo-cortical circuit and its connections to the basal ganglia (van der Stouwe et al., 2020; Nieuwhof et al., 2018). This hypothesis is supported by several lines of research. Stereotactic interventions on the posterior ventral lateral nucleus of the thalamus (VLp, also referred to as VIM), a cerebellar relay nucleus, as well as DBS of the internal globus pallidus (GPi) or one of its thalamic relay nuclei (the ventral lateral anterior nucleus (VLa), also referred to as VOp), can both suppress tremor in dystonia (Cury et al., 2017; Hedera et al., 2013; Tsuboi et al., 2020; Sobstyl et al., 2020; Fasano et al., 2017; Tsuboi et al., 2021). Furthermore, functional MRI during a grip-force task has been used as a proxy of tremor-related cerebral activity (DeSimone et al., 2019), showing similar grip-force related activity in the cerebellum between dystonic tremor and essential tremor. Since cerebellar dysfunction is well-established in essential tremor (Broersma et al., 2016; Buijink et al., 2015; Pan et al., 2020; Gallea et al., 2015), this suggests that cerebellar dysfunction may also play a role in dystonic tremor syndromes. In the same study, dystonic tremor was associated with reduced functional connectivity of the VLp, GPi, and dentate nucleus (DeSimone et al., 2019). In two other functional MRI studies, patients with dystonic voice tremor had increased cerebellar activity during speech production (Kirke et al., 2017) and reduced self-inhibition of the putamen during rest (Battistella and Simonyan, 2019). However, these previous studies did not directly relate altered brain activity to tremor, which limits the conclusions that can be drawn. In a structural MRI study, dystonic tremor patients had an increased grey matter volume (GMV) in the sensorimotor cortex when compared to controls and essential tremor patients (Cerasa et al., 2014), hinting at cortical rather than subcortical mechanisms. Finally, classical eye blink conditioning and temporal somatosensory discrimination, which are markers for cerebellar and basal ganglia dysfunction, respectively, are affected in patients with dystonic tremor syndromes (Antelmi et al., 2016; Conte et al., 2018). Taken together, these findings suggest that both the cerebello-thalamo-cortical circuit and the basal ganglia are involved in dystonic tremor syndromes, but direct evidence is lacking, and the role of each circuit remains unclear.

Here, we aimed to identify the cerebral circuit underlying dystonic tremor syndrome, by focusing on specific patterns of tremor-related activity independent of voluntary movements (such as posture holding). We combined accelerometery with functional MRI, using the same method as previously applied to Parkinson's disease tremor (Dirkx et al., 2020), Holmes tremor (Nieuwhof et al., 2020) and essential tremor (Buijink et al., 2015). We disentangled cerebral activity related to hand lifting, posture holding, and hand lowering from cerebral activity related to fluctuations in tremor amplitude. We hypothesized to find tremor-related activity in the cerebello-thalamo-cortical circuit and the basal ganglia (specifically, the GPi), possibly as a function of structural changes and/or clinical tremor characteristics. Finally, within the tremor-related network, we investigated the role of inter-regional connections in the generation of dystonic tremor syndrome. To this end, we used dynamic causal modelling to test where cerebral activity first arises during hand-lifting, and which connections are related to fluctuations in tremor amplitude.

2. Materials and methods

2.1. Participants

We included 27 patients with dystonic tremor syndrome from the Radboud university medical centre (Radboudumc Nijmegen, 18 patients), Academic Medical Center (AMC Amsterdam, 7 patients), Maastricht University Medical Center+ (MUMC Maastricht, 1 patient) and Canisius Wilhelmina Ziekenhuis (CWZ Nijmegen, 1 patient). For comparison of grey matter volume with patients, we selected 27 healthy controls from two prior studies that best matched our dystonic tremor syndrome group on age and sex (Nuland et al., 2020; Lustenhouwer et al., 2019). The healthy controls were 61.0 ± 11.5 years old (range 34–80) and sex was distributed as in dystonic tremor syndrome patients (13 male, 14 female). Inclusion criteria for dystonic tremor syndrome patients were a clinical diagnosis of dystonic tremor or tremor associated with dystonia, with the presence of primary focal or segmental dystonia, according to the most recent consensus statement (Bhatia et al., 2018). Patients with questionable dystonia and bilateral, sinusoidal, highly regular (in amplitude and rhythm) postural tremor were classified as essential tremor plus and excluded from this study (Bhatia et al., 2018; Pandey et al., 2020).

Exclusion criteria for all participants were: MRI contraindications, a history of traumatic brain injury or stroke, moderate to severe head tremor when lying supine, cognitive dysfunction (defined as a clinical diagnosis of mild cognitive impairment or dementia), and the use of anti-tremor medication other than propranolol. All participants participated voluntarily and gave their written informed consent prior to starting the study. The study was approved by the ethical committee 'Commissie mensgebonden onderzoek (CMO) regio Arnhem-Nijmegen' and was performed according to the principles of the Declaration of Helsinki. Propranolol was tapered off for the patients using it ($n = 10$) in the week prior to measurements so all measurements were done in the off-medication state. To prevent any effect of botulinum toxin treatment, measurements for the two patients who received injections in the most tremulous arm were scheduled three and six months after the latest injection.

2.2. Experimental procedures and paradigm

Patients visited our lab on two separate sessions. During the first visit, we performed a clinical examination and videotaped this for later review and confirmation of diagnosis by two experienced neurologists (RH and BvdW). Table 1 provides details on the clinical testing. Using functional MRI, we scanned participants during both the first and the second visit ($n = 15$) or during one of the visits ($n = 12$). During scanning, we used a block design to evoke postural tremor while allowing sufficient periods of rest (20 blocks of 30 s posture holding alternated with 20 blocks of 9–11 s rest, in total 13.3 min). Specifically, we asked participants to rest their hands and arms on their hip or the scanner bed whenever the text 'RUST' (Dutch for rest) was displayed. When 'STREK' (Dutch for stretch) was displayed, we asked participants to assume an individually defined tremor-evoking posture with the arm that was most affected by tremor.

Table 1
Characteristics of participants.

	Dystonic tremor syndrome (N = 27) mean ± std (range)
General	
Age (years)	62.0 ± 12.7 (28.0–82.0)
Sex (M/F)	13/14
FAB	16.2 ± 1.9 (11.0–18.0)
MOCA	26.8 ± 2.9 (19.0–31.0)
Tremor	
Most affected arm (left/right)	11/16
Postural tremor frequency (Hz)	5.7 ± 1.6 (3.8–9.4)
TRS total score	41.8 ± 15.8 (18.0–84.0)
TRS most affected hand	17.0 ± 5.3 (8.0–26.0)
Tremor duration (years)	24.1 ± 15.6 (8.0–58.0)
Tremor response to alcohol (0-no response, 100-full tremor suppression)	19.6 ± 28.1 (0.0–100.0)
Propranolol usage for tremor (yes/no)	10/17
Head tremor (yes/no)	9/18
Rest tremor (yes/no)	25/2
Kinetic tremor (yes/no)	27/0
Irregular tremor (yes/no)	16/11
Asymmetric tremor (yes/no)	20/7
Position-dependent tremor (yes/no)	18/9
Unilateral tremor (yes/no)	3/24
Dystonia	
BFM total score	7.9 ± 6.7 (0.5–27.5)
Cervical dystonia (yes/no)	23/4
Most tremulous arm dystonia (yes/no)	23/4
Least tremulous arm dystonia (yes/no)	17/10
Speech/swallow dystonia (yes/no)	5/22
Eyes dystonia (yes/no)	1/26
Leg dystonia (yes/no)	2/25
Trunk dystonia (yes/no)	7/20
Mouth dystonia (yes/no)	0/27

The Fahn-Tolosa-Marin Tremor Rating Scale (TRS) parts A, B and C were assessed for clinical tremor severity (possible ranges 0–88, 0–36 and 0–28 (Stacy et al., 2007). The sum score for items covering the most tremulous hand was calculated and used as measure for tremor severity of the most affected hand (possible range 0–28). Peak tremor frequency and the effect of weighing were assessed by using accelerometery. The Burke-Fahn-Marsden rating scale (BFM, possible range 0–120) was used for severity of dystonia (Burke et al., 1985), the Montreal Cognitive Assessment (MOCA, possible range 0–31) score for general cognitive functioning (Hoops et al., 2009; Nasreddine et al., 2005), the Frontal Assessment Battery (FAB, possible range 0–18) for frontal lobe functioning (Dubois et al., 2000; van Loo et al., 2007).

2.3. Tremor analysis

During scanning, we recorded tremor by using an MRI-compatible tri-axial accelerometer (Brain Products; sampling frequency *(Fs)* = 5 kHz) (Dirkx et al., 2016). We placed the accelerometer on the location where tremor was best captured (dorsum of the hand or one of the fingers). Accelerometery data was detrended and demeaned. We then segmented the data into 5 s segments over which we calculated power spectra with 0.2 Hz spectral resolution. These power spectra were averaged and used to determine the channel and frequency with highest tremor power. We then calculated the time–frequency representation of this channel between 2 and 18 Hz. For this, we used a Hanning taper with a window length equal to 8 periods at peak tremor frequency (e.g. 2 s for 4 Hz tremor) to minimize spectral leakage. From this, we extracted the tremor power time-course at each individual's peak tremor frequency (Fig. 1). This time course was down sampled to the repetition time to obtain scan-to-scan tremor power.

2.4. MRI image acquisition and pre-processing

MRI images were acquired on a Siemens PRISMA 3 T MRI system, using a 64-channel head-neck coil. T2*-weighted images were obtained using multiband echo planar imaging (EPI), with multiband acceleration factor 6, repetition time 1 s, echo time 34 ms, 2.0 mm isometric voxels, 72 slices and a field of view of 210 mm. A high-resolution anatomical image was acquired using an MP-RAGE (magnetization-prepared rapid gradient-echo) sequence for both patients and healthy controls (repetition time 2300 ms, echo time 3.03 ms, voxel size 1.0 mm isometric, 192 sagittal slices, field of view 256 mm). Functional images were pre-processed using previously described procedures with a net smoothing kernel of 6 mm (Dirkx et al., 2020). This included ICA-AROMA (independent component analysis-based automatic removal of motion artefacts) for automatic classification and removal of noise components (Pruim et al., 2015; Pruim et al., 2015). Since ICA-AROMA was developed for resting-state data, the automatic classification was manually checked and corrected to prevent signal at task or tremor frequency to be inadequately classified as noise. We added movement parameters to our first level design to ensure this procedure did not reintroduce movement artefacts, which can resemble signal of interest. We normalized functional images to MNI (Montreal Neurological Institute) space and, for optimal sensitivity in the cerebellum, to a cerebellum specific template using the SUIT toolbox (Diedrichsen, 2006).

2.5. Functional MRI analysis

For each participant, we performed a multiple regression analysis at the first level using the general linear model implemented in SPM12 (Fig. 1). For optimal timing, we manually defined the time points of hand lifting and lowering based on the raw accelerometery data. We used these time points to model hand lifting and lowering as stick functions. In addition, we modelled posture holding (maintaining the tremor-evoking arm position) per volume, starting 2 s after arm lifting and ending 1 s before arm-lowering. Specifically, we entered onsets at times of volume initiation and durations equal to the repetition time (1 s). We modelled fluctuations in tremor power by adding scan-to-scan tremor power as parametric modulation to these posture holding volumes. This allowed us to detect fluctuations in cerebral activity associated with fluctuations in tremor power, independent from cerebral activity related to posture holding, hand lifting or hand lowering. A similar approach has been used before (Dirkx et al., 2020). For removal of non-neural noise and motion artefacts we added the average time course of the bilateral ventricles and 36 movement parameters (Volterra expansion: translation and rotation of 3 axes, original and first derivative, linear, quadratic and cubic polynomials) as nuisance regressors (Lund et al., 2005). We averaged over sessions at the first level for participants who performed the task during both sessions (N = 15, average time between sessions 5.5 ± 3.8 months). Two sessions with a maximum scan-to-scan displacement > 3 mm were excluded from analyses (for two participants who both had another session with less displacement). Mean scan-to-scan displacement was 0.14 ± 0.07 mm (range 0.06–0.37 mm) and maximal scan-to-scan displacement was 0.94 ± 0.68 mm (range 0.21–2.64 mm). Parameter estimates for all regressors were obtained by restricted maximum-likelihood estimation, and a temporal high pass filter with 128 s cut-off was used.

First-level contrast images were taken to the second level and entered into one-sampled t-tests. For participants with most severe tremor at the left hand (N = 11), we flipped the contrast images in the axial plane (both for whole brain and cerebellum specific (SUIT) analyses) (Helmich et al., 2011; Dirkx et al., 2016). In this way, the primary motor cortex contralateral to the tremulous arm was always on the left side in the image.

2.6. Effective connectivity: Dynamic causal modelling

The analyses above demonstrated tremor-related activity in nodes of the cerebello-thalamo-cortical circuit (cerebellum, thalamus and BA4) and basal ganglia (GPi). However, it does not specify how these nodes interact with each other (effective connectivity), and most importantly,

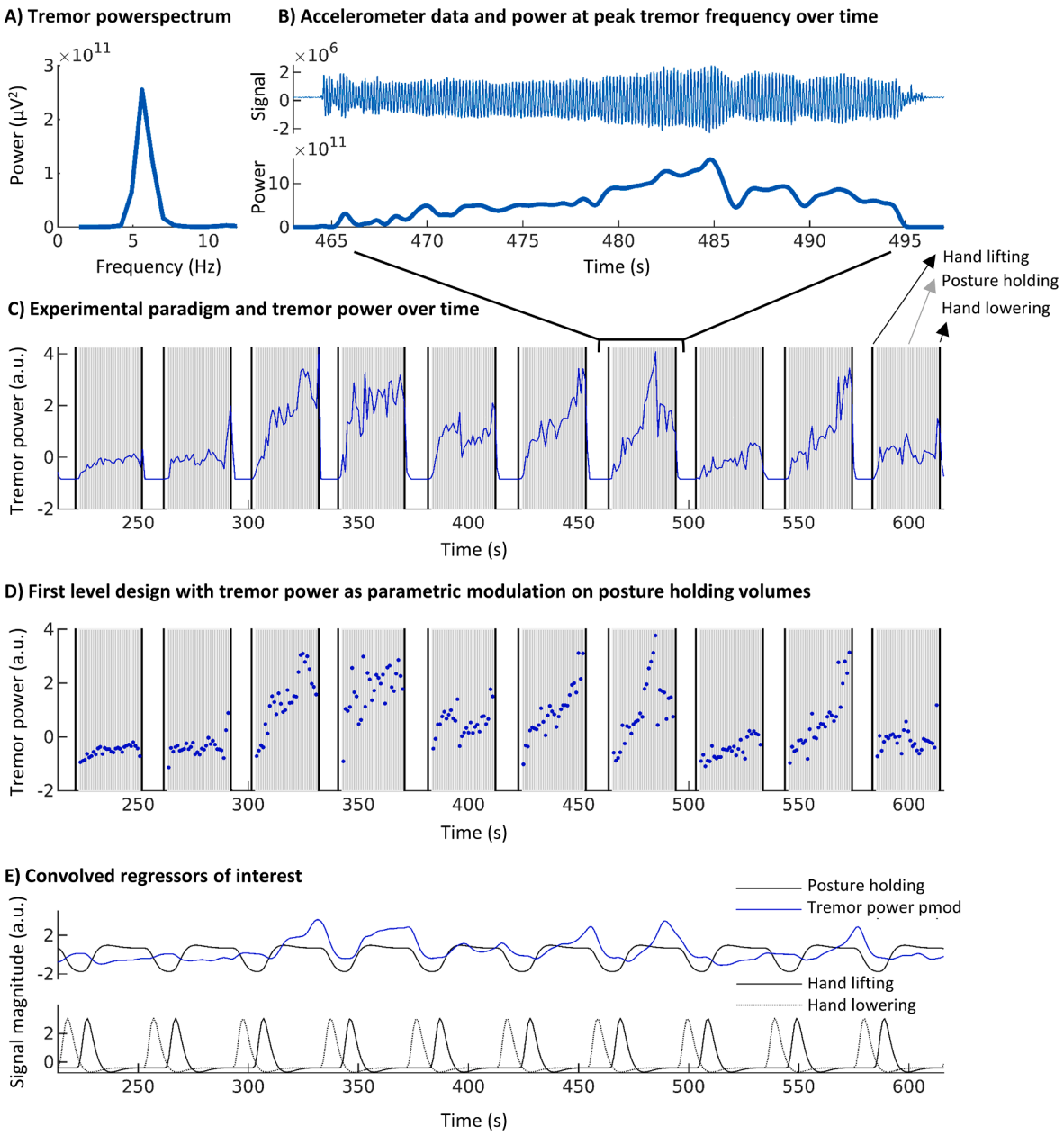

Fig. 1. Tremor analysis and first level design. This figure illustrates the implementation of postural tremor analyses in our fMRI design for a representative participant. **(A)** Average power spectrum over the entire task, used to determine peak tremor frequency **(B)** Accelerometery signal of the axis with highest peak tremor power (top) and corresponding power over time at peak tremor frequency (bottom) for a single block. **(C)** Tremor power over time (blue) plotted over the experimental paradigm that included hand lifting, posture holding and hand lowering (10 out of 20 blocks). Note that, since high amplitude tremor was present during posture holding while only low amplitude tremor was present during rest, tremor power over time and posture holding are positively correlated. **(D)** Implemented first level design which mathematically separated posture holding and tremor power over time. Posture holding was modelled per volume with tremor power as parametric modulation per volume. **(E)** Regressors of interest in the first level design after convolution with the hemodynamic response function. Note that posture holding and tremor power are no longer positively correlated. This model allows for determination of tremor-related activity independent from hand onset, posture holding and hand offset movements. Pmod = parametric modulation. a.u. = arbitrary units. (For interpretation of the references to colour in this figure legend, the reader is referred to the web version of this article.)

how fluctuations in inter-regional coupling are related to fluctuations in tremor amplitude. To investigate this, we used Dynamic Causal Modelling (DCM), which is a Bayesian method of inference where one defines one or more cerebral models based on predefined hypotheses to test for causal influences that one neural system exerts over the other (Friston et al., 2003). Here, we constructed a model space to test: (1) where cerebral activity first arises during hand lifting (aim 1), and (2) which (self)-connections are related to fluctuations in tremor amplitude (aim 2). This approach has been used before for Parkinson's disease tremor (aim 1) (Dirkx et al., 2016) and for essential tremor (aim 2) (Buijink et al., 2015). We used a model with four regions of interests with tremor-related activity: sensorimotor areas of the cerebellum (Buckner et al., 2011), the thalamus, motor cortex (BA4), and GPi (see statistical analysis paragraph for exact ROI definition). We extracted BOLD fMRI timeseries using the first eigenvariate of voxels showing tremor related-activity in these ROIs, adjusting for other effects (i.e. hand lifting, posture holding, tremor, and hand lowering). All intrinsic connections (DCM.A) were based on direct anatomical connections as described in previous work (Dirkx et al., 2016; 2017; 2020). Given that tremor-related activity in the thalamus overlapped both VLp and VLa,

and given that our spatial resolution was insufficient to reliably disentangle these two thalamic nuclei, we considered both cerebellum-thalamus (VLp) and GPi-thalamus (VLa) connections in our model (Fig. 3b). Next, we added hand lifting as a direct input (DCM.C) on the four nodes and tremor amplitude fluctuations (parametric modulator) as modulatory input (DCM.B) on the intrinsic interregional and self-connections. In DCM, self-connections reflect self-inhibition, which is incorporated to ensure decay of activity in the absence of input (Friston et al., 2003). This yielded a total of 4 (direct input on 4 possible nodes) $\times$ 2^{11} (modulatory input on intrinsic connections) = 8,192 models, of which we defined four model families that shared a unique direct input (DCM.C) to one of the four nodes (Penny et al., 2010). We used deterministic DCM 12.5 for all our analyses.

We used random effects Bayesian model selection to determine which of the four model families most likely generated the observed BOLD responses (Stephan et al., 2010). Next, we applied Bayesian model averaging to calculate mean parameters of the winning model family considering the relative model evidence (Penny et al., 2010; Stephan et al., 2010). We tested DCM.B parameters using one-sample two-tailed t-tests against zero (FDR corrected for 11 comparisons) to investigate significant associations between effective connectivity and tremor amplitude fluctuations. Significant parameters were correlated with clinical tremor severity (sum score of TRS items of the most affected hand) and dystonia severity (Burke-Fahn-Marsden; BFM) using Bayesian Pearson's r correlation coefficients (Ly et al., 2016; Ly et al., 2018) (H0 = correlation absent, H1 = correlation present).

2.7. Structural MRI analysis

We tested for structural brain changes in dystonic tremor syndrome patients using voxel-based morphometry (VBM). Structural images were segmented into grey matter, white matter, and cerebrospinal fluid. Grey matter images were normalized to Montreal Neurological Institute (MNI) space and the Cerebellar template (SUIT) via a study specific template by using Diffeomorphic anatomical registration through exponentiated lie algebra (DARTEL) (Ashburner, 2007). We applied a 6 mm smoothing kernel. We entered the processed grey matter images in a two-sample *t*-test to compare grey matter volume (GMV) between dystonic tremor syndrome patients and controls. We added age and gender as covariates and corrected for brain volume differences by dividing voxel-by-voxel intensities by total intracranial volume (ICV).

2.8. Regions of interest

Given our a-priori hypothesis on involvement of both the cerebello-thalamo-cortical circuit and the basal ganglia (GPi) in dystonic tremor syndrome, we focused our analyses on these regions. The anatomical regions of interest we used were the cerebellum (using the SUIT toolbox), the GPi (taken from the Basal Ganglia Human Area Template toolbox (Prodoehl et al., 2008), Brodmann Area 4 (BA4, taken from the WFU PickAtlas (Maldjian et al., 2003; 2004)) and a combined mask of the thalamic posterior ventral lateral nucleus (VLp) and anterior ventral lateral (VLa) nucleus, taken from the Morel Atlas (Niemann et al., 2000; Mai and Majtanik, 2018). These thalamic nuclei are common targets for neurosurgical interventions for tremor (Tsuboi et al., 2020; 2021). The Morel atlas uses the thalamic nomenclature as proposed by Jones (Hirai and Jones, 1989), which we will follow in this paper. This nomenclature is an alternative for the nomenclature proposed by Hassler, which is common among clinicians and neurosurgeons. Jones' VLp is thought to correspond largely to Hassler's ventral intermediate nucleus (VIM) (Krack et al., 1997), which receives input from the cerebellum. The VLa corresponds largely to Hassler's ventro-oralis posterior nucleus (VOp), which receives input from the pallidum (Tsuboi et al., 2021; Hutchison et al., 1997; Percheron et al., 1996; Helmich et al., 2012). We used bilateral GPi, BA4 and thalamus ROIs in the structural analyses and unilateral left GPi, BA4 and thalamus ROIs in the functional analyses (matching the flipped functional contrast images).

2.9. Statistical analyses

For the analyses on task and tremor-related activity and the structural analyses, we assessed statistical significance with non-parametric permutation tests using the Threshold Free Cluster Enhancement (TFCE) Toolbox in SPM12 (http://dbm.neuro.uni-jena.de/tfce/) with 10,000 permutations. TFCE circumvents the problem of arbitrarily defined cluster forming thresholds while maintaining sensitivity with use of spatial neighbourhood information (Smith and Nichols, 2009). TFCE values represent the magnitude of evidence at each voxel combined with local spatial support. After TFCE, a voxel-level FWE-corrected p-value < 0.05 was used as threshold for statistical significance inference. We increased this threshold to $p < 0.001$ FWE-corrected for cerebellum-specific tremor-related activity and for hand lifting and lowering-related activity, to increase specificity in those analyses. With TFCE, we tested for tremor-related activity and grey matter volume differences in our regions of interest (ROI) and across the whole brain. The anatomy toolbox (Eickhoff et al., 2005) was used to anatomically localize clusters of activity.

For voxels with significant results, we related our findings with clinical tremor severity (sum score of TRS items of the most affected hand) and dystonia severity (Burke-Fahn-Marsden; BFM). For this, we averaged tremor-related activity and grey matter volume over significant voxels within ROIs using Marsbar (Brett et al., 2002) (see Supplementary Table 2 for included ROIs). Given the predominant tremor-related activity in sensorimotor areas of the cerebellum (Buckner et al., 2011), we averaged over significant voxels in these areas for the cerebellum. We related tremor-related activity to clinical measures using Bayesian Pearson's r correlation coefficients (Ly et al., 2016; Ly et al., 2018) (H0 = correlation absent, H1 = correlation present). For the structural analyses, we considered tremor frequency next to tremor severity and dystonia severity, since structural changes have previously been associated with tremor frequency (Gallea et al., 2015; Deuschl et al., 1999). We applied Bayesian ANCOVA's (Rouder et al., 2012) with these clinical measures as dependent variables and compared which of two models best fitted the data: a model with only age and gender as covariates (the null model) or an alternative model including age, gender and adjusted GMV (GMV/ICV, H0 = best fit of null model, H1 = best fit of alternative model). For the thalamus ROI, which showed both tremor related activity and increased GMV in patients, we tested whether these two measures correlated. We extracted adjusted GMV from the most tremulous side and entered this, as above, in a Bayesian ANCOVA model comparison with tremor-related activity (average beta over thalamus ROI) as dependent variable. Finally, we correlated tremor-related activity (Bayesian Pearson's r correlation) between the different regions of interest, to explore whether a trade-off between brain regions was present (e.g. relatively more cerebellum involvement in some patients and more pallidum involvement in others). All Bayesian analyses were performed in JASP (JASP Team (2019). JASP (Version 0.11.1) [Computer software]). Bayes factors were interpreted according to the guidelines provided in JASP (Wagenmakers et al., 2018), in which Bayes factors (BF_{10}) of 1–3, 3–10 or > 10 are considered anecdotal, moderate or strong evidence for the alternative hypothesis, while BF_{10} of 0.33–1, 0.1–0.33 or < 0.1 are considered anecdotal, moderate or strong evidence for the null hypothesis.

3. Results

Characteristics of dystonic tremor syndrome patients are presented in Table 1. Posture holding significantly increased tremor power (posture holding vs. non-posture holding, log tremor power 9.0 $\pm$ 1.2 versus 6.2 $\pm$ 0.6, $t_{(26)} = 11.02$, $p < 0.001$, Supplementary Fig. 1). The majority of patients (85%, $n = 23$) were diagnosed as dystonic tremor (dystonia in tremulous hand/arm), and 15% ($n = 4$) as tremor associated

with dystonia (dystonia in body part other than tremulous hand/arm). Tremor was judged to be slightly irregular in 59% of patients, asymmetrical in 74%, and posture-dependent in 67%. None of the patients had myoclonus.

3.1. Tremor-related brain activity

We observed significant tremor-related activity in the cerebellum, pallidum and thalamus, bilateral frontal pole, and small clusters in the brainstem and temporal pole (whole brain analysis, Fig. 2, Table 2). ROI analyses revealed that tremor-related activity was most pronounced in sensorimotor regions of the cerebellum, i.e. right lobule I-IV and V, right crus I&II, vermis VI and VIIIa, and left lobules I-IV and V (Buckner et al., 2011) (Table 2). When testing in our other three ROIs, we found significant tremor-related activity in the left GPi (15 voxels, MNI local maximum [−18 −8 −4], *TFCE* = 71.35, *p(fwe)* = 0.005), the left

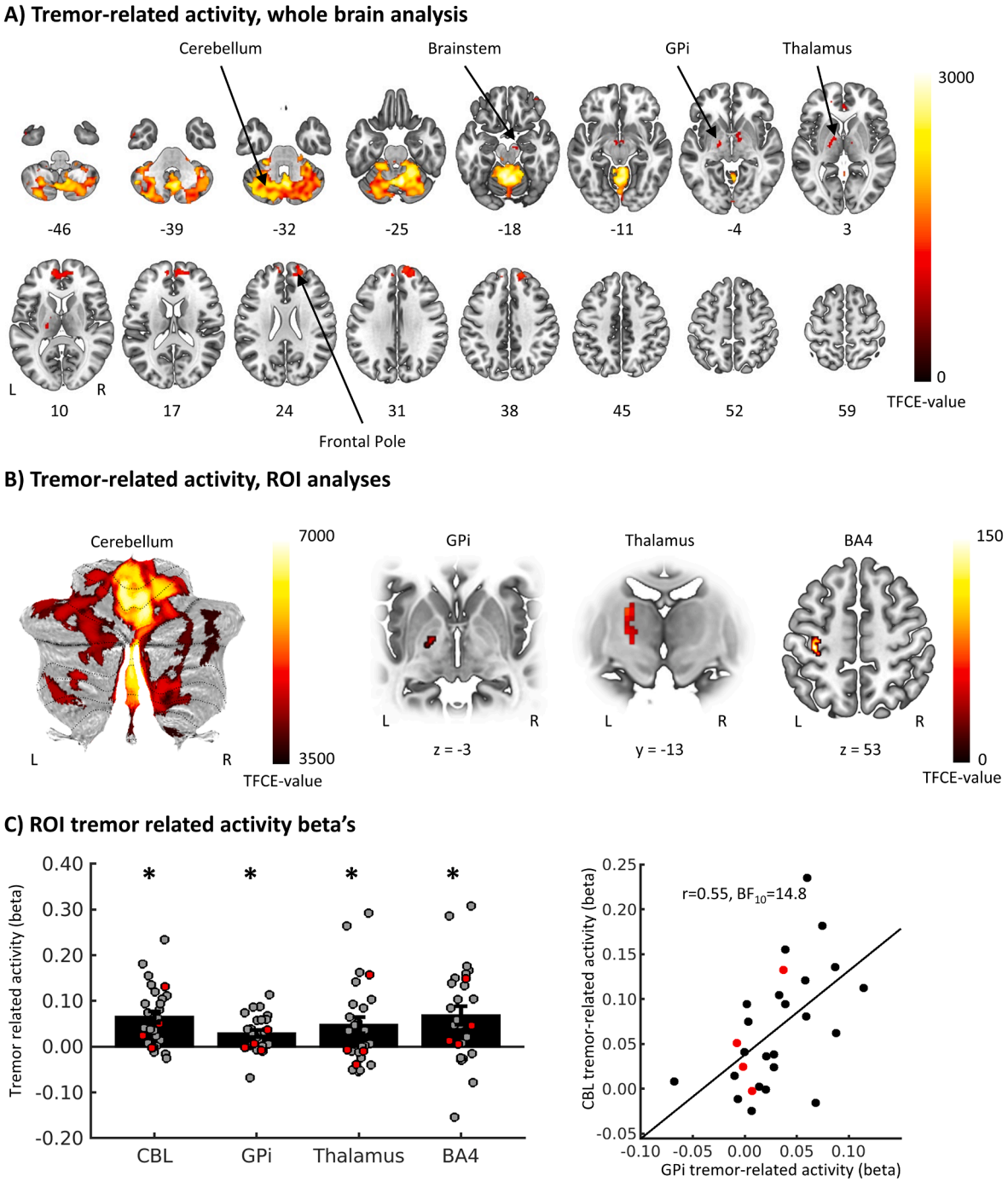

Fig. 2. Tremor-related activity. (A) Brain regions with significant tremor-related activity in the whole brain analysis. Values represent z-axis MNI coordinates. **(B)** Voxels with significant tremor related activity in the region of interest analyses. **(C)** Tremor-related activity averaged over significant voxels in the somatomotor regions of the cerebellum, the GPi, Thalamus (VLp and VLa) and BA4 (left plot). Bars represent mean beta values (±SEM), dots represent individual beta's and asterisks indicate statistical significance. The right plot shows a positive correlation between cerebellar and GPi tremor related activity. Patients with dystonic tremor are displayed in grey/back dots, patient with tremor associated with dystonia in red dots. GPi = internal globus pallidus, TFCE = Threshold free cluster enhancement, ROI = Region of interest, VLp = posterior ventral lateral nucleus, VLa = anterior ventral lateral nucleus, BA4 = Brodmann Area 4, CBL = Cerebellum, L = left, R = right. (For interpretation of the references to colour in this figure legend, the reader is referred to the web version of this article.)

Table 2
Tremor related activity.

Region	Side	Cluster size (number of voxels)	P_{FWE}	TFCE-value	Coordinates peak voxels		
					x	y	z
Whole brain analysis							
Cerebellum	L + R	15,519	<0.001	3081	−4	−54	−16
			<0.001	3022	8	−62	−26
			<0.001	3005	6	−58	−18
Pallidum	L	686	0.031	1234	−16	−8	−4
			0.032	1224	−16	−4	4
Thalamus	L		0.038	1158	−20	−16	6
			0.038	1157	−22	−20	8
			0.039	1139	−16	−6	12
Pallidum	R		0.042	1115	14	−4	−4
Thalamus	R		0.046	1080	12	−8	6
			0.046	1078	16	−6	10
			0.047	1072	18	−14	10
Frontal Pole	R	1677	0.021	1387	14	60	30
			0.022	1380	16	52	38
			0.023	1363	20	56	24
	R	48	0.038	1157	38	50	−18
	R	2	0.049	1047	38	48	−8
Frontal Pole	L	6	0.049	1055	−18	52	16
Brainstem	R	74	0.041	1118	12	−16	−16
Temporal Pole	L	113	0.026	1314	−54	2	−38
Cerebellum specific analysis							
Right Lobule I_IV / V	R	31,149	<0.001	6772	8	−61	−26
			<0.001	6687	7	−57	−19
			<0.001	6184	20	−53	−23
Vermis VI / VIIIa	medial		<0.001	6568	0	−62	−29
			<0.001	6188	2	−65	−34
			<0.001	6186	5	−66	−39
Left Lobule I_IV / V	L		<0.001	6703	−4	−54	−13
			<0.001	6696	−5	−58	−16
			<0.001	6677	−4	−62	−16
			<0.001	6076	−5	−47	−17
Right_Crus I & II	R	570	0.001	3811	43	−57	−45
			0.001	3796	44	−62	−35
			0.001	3670	37	−63	−41

thalamus (88 voxels, MNI local maximum [-18 –16 12], *TFCE* = 77.05, *p (fwe)* = 0.012) and the left BA4 (hand area of the primary motor cortex, 130 voxels, MNI local maximum [−36 –26 56], *TFCE* = 151.88, *p(fwe)* = 0.002), see Fig. 2B. Within the thalamus, tremor-related activity could be localized to both the VLp (27.63% of the dorsal VLp and 31.22% ventral VLp were activated) and the VLa (69.91% activated). Tremor-related activity did not differ between the thalamic nuclei (mean beta over whole VLa = 0.045 ± 0.096, VLpv = 0.040 ± 0.096 and VLpd = 0.043 ± 0.107, one-way repeated measures ANOVA *F(2,52)* = 0.144, *p* = 0.866). Tremor-related activity did not correlate with clinical tremor severity or dystonia severity in any of the ROIs (Supplementary Table 2, All $BF_{10} < 1$, anecdotal to moderate evidence for H0). Tremor-related activity in the cerebellum showed a positive correlation with tremor-related activity in the GPi (Fig. 2C and Table 3, $BF_{10} = 14.8$, strong evidence for H1).

Table 3
Correlation coefficients of tremor-related activity between ROIs.

	Cerebellum	GPi	VLp	BA4
Cerebellum	–			
GPi	0.546 (14.8)	–		
Thalamus	0.820 (>100)	0.679 (48.4)	–	
BA4	0.778 (>100)	0.515 (8.7)	0.687 (>100)	–

Values displayed as: Pearson's r (Bayes Factor BF_{10}).

3.2. Hand-lifting related brain activity

By design, tremor-related activity was specific to fluctuations in tremor power and not associated with hand lifting, posture holding, or hand lowering. Hand lifting and hand lowering were associated with a specific pattern of activity in the contralateral sensorimotor cortex and ipsilateral cerebellum (laterality related to the used hand), as well as a more widespread motor circuit during hand lowering. Furthermore, stable posture holding, defined as holding the hand in the predefined posture, was related to brain activity in the ipsilateral cerebellum. See Supplementary Table 1 and Supplementary Fig. 2 for more (statistical) details.

3.3. Effective connectivity

Bayesian model selection revealed that during hand lifting, which coincides with the onset of tremor, network activity most likely starts in BA4, rather than in the cerebellum, thalamus or GPi (highest probability for an input [DCM.C] onto BA4: expected posterior probability = 0.43, exceedance probability = 0.83, Fig. 3a). Furthermore, Bayesian model averaging showed that connectivity from the cerebellum to thalamus (*DCM.B* = 0.60 ± 0.08 Hz, *t(26)* = 2.92, *p(FDR-corrected)* = 0.039) and the thalamus inhibitory self-connection (*DCM.B* = 1.35 ± 0.09 Hz, *t(26)* = 4.12, p(FDR-corrected) = 0.004) were positively modulated by tremor amplitude fluctuations (Fig. 3 B,C). These effects were not observed for connectivity between the GPi and thalamus or any other region (*p(FDR-corrected)* > 0.05). This suggests that individual fluctuations in tremor amplitude are specifically driven by cerebello-thalamic connectivity. These connectivity parameters were not correlated with clinical tremor or dystonia severity (Supplementary Table 2, all $BF_{10} < 3$, never exceeding anecdotal evidence for H1).

3.4. Grey matter volume

ROI analyses showed significantly increased grey matter volume in patients versus controls in BA4 (two bilateral medial clusters and a left lateral cluster) and in the left thalamus (Table 4, Fig. 4). Within the thalamus, increased grey matter volume was localised in VLp (49.74% of the dorsal VLp and 24.50% of the ventral VLp showed increased grey matter volume) and the VLa (28.84% of the VLa with increased grey matter volume). Within the thalamus, there was an overlap between voxels showing tremor-related activity and voxels showing increased grey mater volume. In contrast, in BA4 the region showing increased grey matter was located more medially than the region showing tremor-related activity, without overlap. Grey matter volume in these clusters did not correlate with clinical tremor severity, dystonia severity or tremor frequency (except for moderate evidence for a positive correlation between GMV in medial BA4 and tremor frequency, Supplementary Table 3). In the thalamus, grey matter volume did not correlate with tremor-related activity (Pearson's r = 0.08, $BF_{10} = 0.57$). Whole brain analyses revealed no other regions showing significant group differences.

4. Discussion

We investigated cerebral activity associated with tremor in dystonia. To this end, we disentangled cerebral activity specifically related to tremor fluctuations from activity related to (voluntary) posture holding. There are three main findings. First, tremor-related activity was present in both the cerebello-thalamic-cortical circuit (motor regions of the cerebellum, thalamus (VLp), hand area in the primary motor cortex), and in the basal ganglia (GPi, as well as the pallidal recipient thalamic nucleus VLa). Second, effective connectivity from cerebellum to

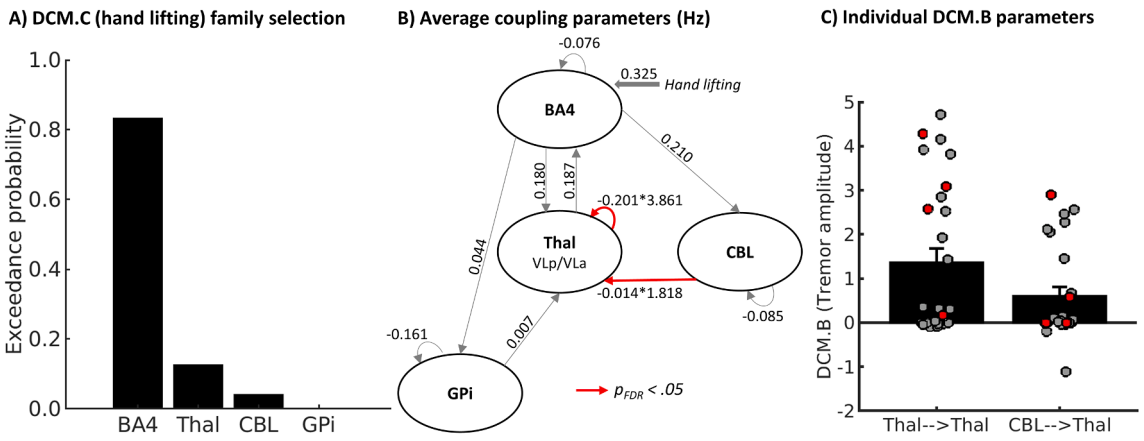

Fig. 3. Results of dynamic causal modelling. (A) Bayesian model selection comparing families of models with input of hand lifting (DCM.C) on BA4, Thalamus, Cerebellum or GPi **(B)** Mean coupling parameters resulting from Bayesian model averaging over all models with input of hand lifting on BA4. Intrinsic connectivity parameters (DCM.A) are displayed for all connections. For connection with significant modulation of tremor amplitude (Cerebellum to thalamus and thalamus self-connection) the net coupling parameters are calculated according to DCM.A*exp(DCM.B). **(C)** Individual DCM.B parameters for connections with significant modulation of tremor amplitude. Patients with dystonic tremor are displayed in grey/back dots, patient with tremor associated with dystonia in red dots. BA4 = Brodmann Area 4, Thal = Thalamus, CBL = Cerebellum, GPi = internal globus pallidum, FDR = False discovery rate. (For interpretation of the references to colour in this figure legend, the reader is referred to the web version of this article.)

Table 4
Grey matter volume differences between dystonic tremor patients and healthy controls, region of interest analyses.

Region	Side	Cluster size (number of voxels)	P_{FWE}	TFCE-value	Coordinates peak voxels		
					x	y	z
BA4 patients > controls							
Medial BA4	Left	670	<0.001	825	−11	−22	73
			0.001	687	−19	−23	72
			0.040	268	−30	−16	72
Medial BA4	Right	840	0.008	457	14	−20	73
			0.014	390	9	−25	77
			0.039	270	24	−25	72
Lateral BA4	Left	454	0.016	373	−48	−5	56
			0.034	288	−50	−3	46
Thalamus patients > controls							
Thalamus (VLp/VLa)	Left	659	0.020	221	−15	−14	1
			0.021	218	−17	−13	14

thalamus and thalamus self-inhibition were associated with tremor amplitude fluctuations. Third, grey matter volume was increased in patients compared to controls, in the same thalamic region showing tremor-related activity (both VLp and VLa), and in two regions within the primary motor cortex where we did not observe tremor-related activity (bilateral medial and left lateral BA4). Below we discuss how these findings help to understand the complex pathophysiology underlying dystonic tremor syndromes.

4.1. Dystonic tremor syndrome: The role of the cerebello-thalamo-cortical circuit

We confirmed our hypothesis that both the cerebello-thalamic circuit and the basal ganglia are involved in dystonic tremor syndrome, although the extent of tremor-related activity in the cerebellum was much larger than in the other regions. In contrast to the pronounced tremor-related activity in the cerebellum, tremor-related activity in BA4 was only observed in a ROI analysis, and it was less extensive. This may suggest that dystonic tremor syndrome is driven by subcortical more than cortical mechanisms. This fits with behavioural findings suggesting that the cerebellum plays a key role in the pathophysiology of dystonic tremor syndrome. Specifically, the temporal prediction of motion perception and classical eye blink conditioning, both markers of cerebellar dysfunction, are impaired in dystonia patients with tremor versus without tremor (Antelmi et al., 2016; Martino et al., 2020). Furthermore, in a mouse model of dystonia, blocking of glutamatergic olivocerebellar signalling caused a limb tremor (White and Sillitoe, 2017). The tremor-related activity we observed was specific to fluctuations in tremor, and therefore goes beyond a more general "trait" of dystonia. Nevertheless, the role of the cerebellum in dystonic tremor syndrome, as shown here, aligns with more general ideas that the cerebellum plays a critical role in the pathophysiology of dystonia (Latorre et al., 2020). This is evidenced by functional and structural alterations in the cerebellum and its connections to thalamus and primary motor cortex (Hallett et al., 2020). Here we did not find evidence for cerebellar atrophy in dystonia patients, in line with previous work (Gallea et al., 2018). This suggests that the role of the cerebellum in dystonic tremor syndrome is associated with functional rather than structural changes. A possible mechanism underlying tremor-related activity in the cerebellum could be a loss of inhibition due to impaired GABAergic transmission. More specifically, a PET study has shown that focal hand dystonia patients showed a lower flumazenil binding potential than controls in the vermis VI of the ipsilateral cerebellum and the contralateral sensorimotor cortex (with respect to the dystonic arm), while there were no differences in the striatum (Gallea et al., 2018).

The functional role of the cerebellum in dystonic tremor syndrome is further qualified by our finding that effective connectivity from cerebellum to thalamus was modulated by tremor amplitude fluctuations. Specifically, we found a negative endogenous connection between cerebellum and thalamus (the DCM.A parameter in Fig. 3), which was positively modulated by intra-individual fluctuations in tremor power (the DCM.B parameter in Fig. 3). This is consistent with findings in a DCM study in essential tremor, which showed the same combination of findings (Buijink et al., 2015). The negative endogenous connection fits the functional anatomy of the cerebello-thalamic pathway, which consists of two projections: an inhibitory connection between Purkinje cells in the cerebellar cortex and the deep cerebellar nuclei, and an excitatory connection between the deep cerebellar nuclei and thalamic nuclei (VLp) (Maas et al., 2020). The positive modulation of this endogenous connection by tremor amplitude, together with widespread tremor-related activity in the cerebellar cortex, suggests that abnormal activity in the cerebellar cortex drives tremor in dystonia through the thalamus. We could not empirically test whether tremor-related activity was

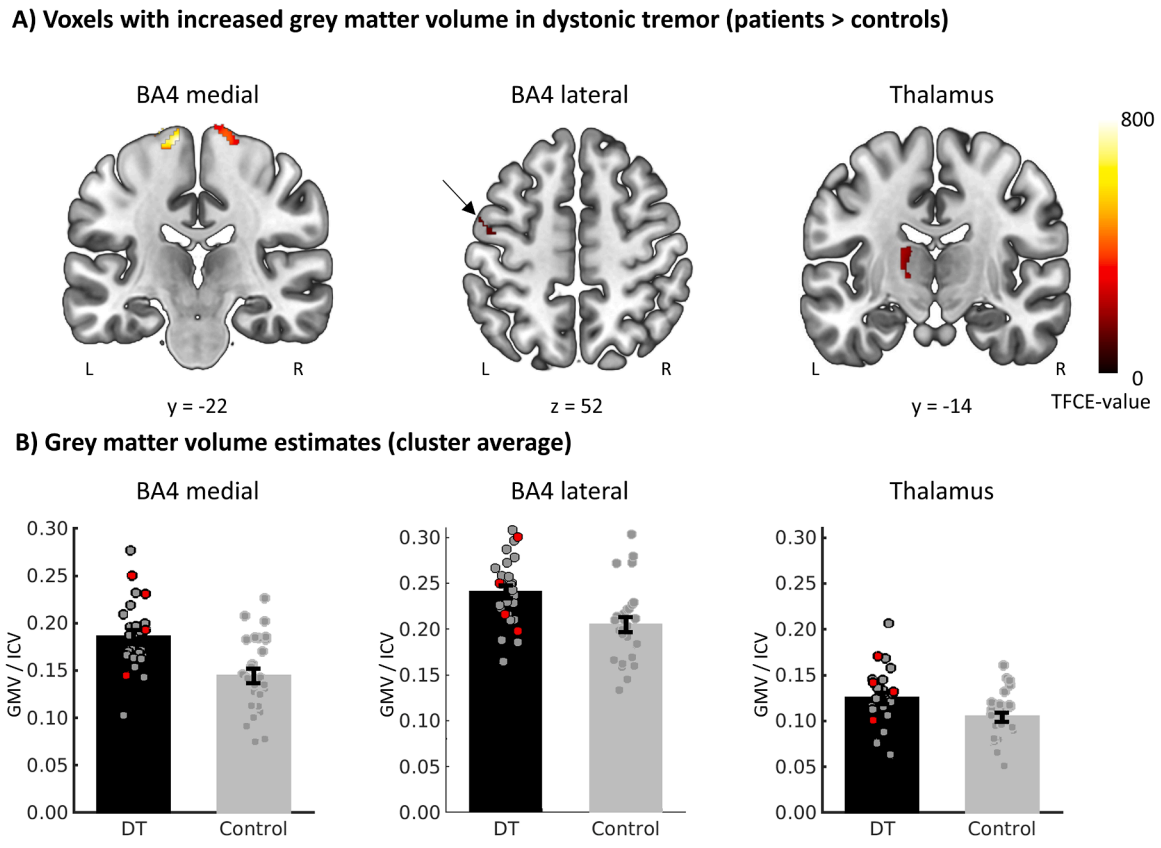

Fig. 4. Grey matter volume differences between dystonic tremor patients and healthy controls. (A) Voxels with significantly higher grey matter volume in dystonic tremor patients compared to controls in region of interest analyses. **(B)** Grey matter volume estimates, adjusted for intracranial volume and averaged over significant voxels displayed in A. Bars represent mean (±SEM) and dots represent individual grey matter volumes. Patients with dystonic tremor are displayed in grey/back dots, patient with tremor associated with dystonia in red dots. BA4 = Brodmann Area 4, TFCE = Threshold free cluster enhancement. GMV = grey matter volume, ICV = Intracranial volume, L = left, R = right. (For interpretation of the references to colour in this figure legend, the reader is referred to the web version of this article.)

indeed initiated in the cerebellum, since the onset of tremor coincides with the onset of hand-movement. Our DCM model comparison showed that, within the tremor circuit, cerebral activity started in BA4 at the onset of movement and/or tremor (Fig. 3: in the winning model family, the DCM.C parameter had its input on BA4). It may well be that these two processes are intertwined, such that dystonic tremor is initiated when an abnormally planned voluntary movement (Delnooz et al., 2013) evokes altered responses in the cerebellum and basal ganglia, resulting in an abnormal cerebello-thalamic drive that then maintains the tremor. To disentangle tremor onset from voluntary movement onset, future research may focus on dystonic rest tremor. The involvement of cerebellum-thalamus connectivity in dystonic tremor syndrome aligns with previous studies. First, DBS for dystonic tremor was successful when targeted at the anatomical connection between cerebellum and thalamus, the dentato-rubro-thalamic tract (Coenen et al., 2020). Second, functional coupling between cerebellum and thalamus was lower in dystonic tremor patients compared to essential tremor patients and controls during a grip-force task (DeSimone et al., 2019). Third, a recent transcranial magnetic stimulation (TMS) study showed that cerebello-cortical inhibition was reduced in patients with dystonic tremor as compared to controls and essential tremor patients (Panyakaew et al., 2020). An unexpected finding is that fluctuations in tremor power were associated with increased (rather than reduced) inhibitory self-connectivity of the thalamus. In Parkinson's disease tremor, dopaminergic medication (which reduces tremor) has previously been shown to specifically increase thalamus inhibition (Dirkx et al., 2017; 2019). In the context of a cerebellar drive, the modulation of tremor amplitude on thalamic self-inhibition can be interpreted as an endogenous attempt to suppress tremor-related activity that arises in the cerebellum. Such self-regulatory mechanisms are thought to be necessary for protecting the brain against non-linear increases in neural activity, which would otherwise result in epileptic seizures. VIM(VLp)-DBS may thus reduce dystonic tremor syndromes (as well as other tremors) by interfering with cerebello-thalamic transmission of tremor oscillations (Coenen et al., 2014), and by potentiating thalamic self-inhibition (Milosevic et al., 2018). The latter hypothesis remains speculative, since we observed a positive instead of a negative correlation between thalamic self-inhibition and tremor severity.

Regional changes in grey matter volume in other nodes of the cerebello-thalamo-cortical circuit in dystonia may further contribute to tremor pathophysiology. That is, although we found no evidence of structural cerebellar alterations in the patients, we did observe increased grey matter volume in the thalamus (in both VLp and VLa) in patients compared to controls. This has previously also been observed in patients with Parkinson's resting tremor (Kassubek et al., 2002), underlining the more general role of the thalamus in tremor. Given that the increase in grey matter in the thalamus overlapped with voxels showing tremor-related activity, it is very likely that the structural changes are related to tremor. Whether these structural changes cause tremor or result from prolonged tremor-related activity (Maguire et al., 2000) remains unknown. In addition, we also found increased grey matter volume in BA4, which aligns with a previous report on cortical thickening in the sensorimotor cortex in dystonic tremor patients compared to controls (Cerasa et al., 2014). The grey matter changes in BA4 did not overlap with tremor-related activity in BA4 and did not correlate with clinical dystonia or tremor severity scores, so it remains unclear whether this

finding is related to the dystonia, to tremor, or both. We observed moderate evidence for a positive relationship between GMV in BA4 and tremor frequency. On the other hand, this (medial) portion of BA4 did not show tremor-related activity, meaning that this effect should be interpreted with caution.

4.2. Dystonic tremor syndrome: The role of the basal ganglia

Besides tremor-related activity in all nodes of the cerebello-thalamo-cortical network, we also found tremor-related responses in the basal ganglia (GPi), and the frontal pole. This underlines that the pathophysiology of dystonic tremor syndrome is not restricted to a single brain region or even a single network, similar to dystonia itself (Latorre et al., 2020; Hallett et al., 2020). The tremor-related activity in the GPi and one of its thalamic relay nuclei (the VLa) suggests involvement of the pallido-thalamic pathway in dystonic tremor syndromes.

This is further supported by a study that reported a sweet spot for DBS in dystonic tremor on the border between VIM (VLp) and VOp (VLa) (Tsuboi et al., 2021). A clinically relevant question is how tremor-related activity in the cerebello-thalamic and the pallido-thalamic pathways relate to each other. The VIM and GPi are two popular targets for tremor suppression with stereotactic surgery (Cury et al., 2017; Hedera et al., 2013; Tsuboi et al., 2020; Sobstyl et al., 2020; Fasano et al., 2017), but treatment is not always effective in reducing dystonic tremor syndrome. For instance, in one study, three out of six dystonic tremor patients first treated with VIM-DBS were subsequently treated with GPi-DBS due to lack of effect (Cury et al., 2017). This may suggest that there is a trade-off between the involvement of the two circuits, where some patients have a "cerebellar-type" tremor and others a "basal ganglia-type" tremor (van der Stouwe et al., 2020; Nieuwhof et al., 2018). Here we found that, across the entire sample, the degree of tremor-related activity in GPi and cerebellum was positively correlated. This goes against the idea of a trade-off, but rather suggests that the basal ganglia and cerebellum act in concert. Specifically, tremor-related activity may be propagated from the cerebellum to the basal ganglia (or vice versa) via reciprocal subcortical anatomical connections between these two structures (Bostan and Strick, 2018), or through the motor cortex – as is the case in Parkinson's resting tremor (Dirkx et al., 2016). Indeed, in patients with cervical dystonia without tremor, abnormal functional connectivity between basal ganglia and cerebellum has been found (Filip et al., 2017). Although beyond the scope of this study, future research could design dedicated DCM models that include the reciprocal connections between cerebellum and basal ganglia and its crucial relay nuclei (i.e. the STN; (Bostan et al., 2010; Bostan and Strick, 2018; Hoshi et al., 2005)) to investigate how these two subcortical regions interact in the context of dystonic tremor syndrome.

We did not find a relationship between the presence or absence of clinical tremor characteristics (such as regularity of the tremor) and the magnitude of tremor-related activity in GPi versus the cerebellum. Support for such differential pathophysiology between tremor phenotypes comes from pallidal single neuron recordings during DBS (Sedov et al., 2020). In pure dystonia and dystonia with jerky head tremor, relatively more burst cells were present, while relatively more pause cells were present in dystonia with sinusoidal head tremor. This suggest that jerky head tremor relies on pallidal alterations, while sinusoidal head tremor relies on other, possibly cerebellar, alterations. Whether this also holds for hand tremor, and which cell types contributed to the BOLD signal we observed, remains unknown. Finally, we also observed tremor-related activity in the frontal pole. This effect might be related to increased cognitive monitoring or arousal during episodes of high-tremor (Dirkx et al., 2020). Future studies with a wider spectrum of tremor phenotypes, including essential tremor, essential tremor plus and dystonic tremor syndrome patients, may further investigate whether there is a gradient between cerebellar and pallidal contributions to tremor depending on the phenotype. Furthermore, studies investigating whether the degree of cerebellar versus pallidal tremor-related activity may predict DBS treatment effects are worthwhile.

4.3. Interpretational issues

First, we did not include a control group for our functional MRI analyses, which raises the question to what extent the findings are specific to dystonic tremor syndrome. We purposely did not include a healthy control group that mimicked tremor, because mimicked (voluntary) and pathological (involuntary) tremor differ in many ways, undermining the value of a direct comparison. For instance, voluntary movements involve motor planning (inverse models) and altered weighing of somatosensory feedback (forward modelling), as compared to involuntary movements (Maurer et al., 2016). Furthermore, mimicked tremor phenotypically differs from pathological tremor in fundamental ways: even in subjects who were explicitly instructed to mimic essential tremor as well as possible, voluntary tremor had a lower frequency and larger wrist extension-flexion movement compared to essential tremor (Broersma et al., 2016). Here, we focused on describing the cerebral tremor network of dystonic tremor syndromes. However, there is considerable clinical overlap between essential tremor, essential tremor plus and dystonic tremor syndromes. A quantitative comparison of tremor-related activity between these tremor types might guide optimal treatment targets for each type and is therefore recommended for future studies. Second, we were unable to show direct correlations between tremor-related activity and clinical tremor or dystonia severity. This raises the question whether the cerebral activity we report is clinically meaningful. On the other hand, it may also suggest that the findings we report are shared across a wide range of dystonia patients with tremor, while larger groups are necessary to detect cerebral sources of inter-individual variability. A third issue we need to consider concerns the included population. We combined patients with dystonic tremor (dystonia in tremulous hand) and with tremor associated with dystonia (dystonia in body part other than tremulous hand). Dystonic tremor was more prevalent than tremor associated with dystonia (85% versus 15% of included patients). This matches the prevalence in a large cohort-study in which 715 patients with dystonic tremor syndrome were included. Of these 715 patients, tremor was classified as dystonic tremor in 614 patients (86%) and as associated with dystonia in 101 patients (14%) (Shaikh et al., 2020). Given that recent findings have indicated pathophysiological differences between DT and TAWD (Panyakaew et al., 2020), we considered the possibility that the 4 TAWD patients in our sample (indicated in red in the figures) may have introduced considerable inter-individual variability. Hence, we repeated our main analyses by including dystonic tremor syndrome subtype (DT versus TAWD) as a covariate. This did not change any of our findings (Supplementary Table 4). Exclusion of the 4 TAWD patients also left our main findings intact (Supplementary Table 4). Although this study was not designed (or powered) to investigate cerebral differences between dystonic tremor syndrome subtypes, the analyses outlined above indicate that the cerebral effects reported here are shared across dystonic tremor syndrome phenotypes.

5. Conclusions

The findings show that both the cerebello-thalamo-cortical circuit and the basal ganglia are involved in the pathophysiology of dystonic tremor syndromes. Specifically, tremor-related activity was present in the cerebellum, the thalamus (VLp and VLa), the primary motor cortex, and the GPi. Given the predominant tremor-related activity in the cerebellum, and altered cerebello-thalamic effective connectivity, we propose that tremor in dystonia may be driven by cerebellar dysfunction. Grey matter hypertrophy of other nodes of the cerebello-thalamo-cortical circuit, i.e. the VLp, VLa, and motor cortex, may further contribute to an imbalance in this network.

CRediT authorship contribution statement

Freek Nieuwhof: Data curation, Formal analysis, Investigation, Methodology, Project administration, Validation, Visualization, Writing – original draft. **Ivan Toni:** Methodology, Resources, Writing – review & editing. **Michiel F. Dirkx:** Methodology, Writing – review & editing. **Cecile Gallea:** Methodology, Writing – review & editing. **Marie Vidailhet:** Methodology, Writing – review & editing. **Arthur W.G. Buijink:** Methodology, Resources, Writing – review & editing. **Anne-Fleur van Rootselaar:** Methodology, Resources, Writing – review & editing. **Bart P.C. van de Warrenburg:** Conceptualization, Funding acquisition, Methodology, Resources, Supervision, Writing – review & editing. **Rick C. Helmich:** Conceptualization, Methodology, Funding acquisition, Supervision, Validation, Writing – original draft, Writing – review & editing.

Declaration of Competing Interest

The authors declare that they have no known competing financial interests or personal relationships that could have appeared to influence the work reported in this paper.

Acknowledgements

We thank all participants and their spouses for investing their time and effort in this study. Also, we thank everybody that helped with recruitment of participants. We acknowledge the funding from the Netherlands Brain Foundation and the Benny Vleerlaag fonds. We thank Renee Lustenhouwer and Annelies van Nuland for their help with data collection.

Appendix A. Supplementary data

Supplementary data to this article can be found online at https://doi.org/10.1016/j.nicl.2021.102919.

References

Defazio, G., Gigante, A.F., Abbruzzese, G., Bentivoglio, A.R., Colosimo, C., Esposito, M., Fabbrini, G., Guidubaldi, A., Girlanda, P., Liguori, R., Marinelli, L., Morgante, F., Santoro, L., Tinazzi, M., Livrea, P., Berardelli, A., 2013. Tremor in primary adult-onset dystonia: prevalence and associated clinical features. J. Neurol. Neurosurg. Psychiatry 84 (4), 404–408. https://doi.org/10.1136/jnnp-2012-303782.

Erro, R., Rubio-Agusti, I., Saifee, T.A., Cordivari, C., Ganos, C., Batla, A., Bhatia, K.P., 2014. Rest and other types of tremor in adult-onset primary dystonia. J. Neurol. Neurosurg. Psychiatry 85 (9), 965–968. https://doi.org/10.1136/jnnp-2013-305876.

Shaikh AG, Beylergil SB, Scorr L, et al. Dystonia & tremor: A cross-sectional study of the dystonia coalition cohort. *Neurology*. Oct 12 2020;doi:10.1212/wnl.0000000000011049.

Bhatia, K.P., Bain, P., Bajaj, N., Elble, R.J., Hallett, M., Louis, E.D., Raethjen, J., Stamelou, M., Testa, C.M., Deuschl, G., 2018. Consensus statement on the classification of tremors. from the task force on tremor of the International Parkinson and Movement Disorder Society: IPMDS task force on tremor consensus statement. Mov. Disord. 33 (1), 75–87.

Wardt, J.V.d., van der Stouwe, A.M.M., Dirkx, M., Elting, J.W.J., Post, B., Tijssen, M.A.J., Helmich, R.C., 2020. Systematic clinical approach for diagnosing upper limb tremor. J. Neurol. Neurosurg. Psychiatry 91 (8), 822–830. https://doi.org/10.1136/jnnp-2019-322676.

Fasano, A., Bove, F., Lang, A.E., 2014. The treatment of dystonic tremor: a systematic review. J. Neurol. Neurosurg. Psychiatry 85 (7), 759–769. https://doi.org/10.1136/jnnp-2013-305532.

Cury, R.G., Fraix, V., Castrioto, A., Pérez Fernández, M.A., Krack, P., Chabardes, S., Seigneuret, E., Alho, E.J.L., Benabid, A.-L., Moro, E., 2017. Thalamic deep brain stimulation for tremor in Parkinson disease, essential tremor, and dystonia. Neurology 89 (13), 1416–1423.

van der Stouwe, A.M.M., Nieuwhof, F., Helmich, R.C., 2020. Tremor pathophysiology: lessons from neuroimaging. Curr. Opin. Neurol. 33 (4), 474–481. https://doi.org/10.1097/WCO.0000000000000829.

Nieuwhof, F., Panyakaew, P., van de Warrenburg, B.P., Gallea, C., Helmich, R.C., 2018. The patchy tremor landscape: recent advances in pathophysiology. Curr. Opin. Neurol. 31 (4), 455–461. https://doi.org/10.1097/wco.0000000000000582.

Hedera, P., Phibbs, F.T., Dolhun, R., Charles, P.D., Konrad, P.E., Neimat, J.S., Davis, T.L., 2013. Surgical targets for dystonic tremor: Considerations between the globus pallidus and ventral intermediate thalamic nucleus. Parkinsonism Related Disord. 19 (7), 684–686. https://doi.org/10.1016/j.parkreldis.2013.03.010.

Tsuboi, T., Jabarkheel, Z., Zeilman, P.R., Barabas, M.J., Foote, K.D., Okun, M.S., Wagle Shukla, A., 2020. Longitudinal follow-up with VIM thalamic deep brain stimulation for dystonic or essential tremor. Neurology 94 (10), e1073–e1084.

Sobstyl, M., Pasterski, T., Aleksandrowicz, M., Stapińska-Syniec, A., 2020. Treatment of severe refractory dystonic tremor associated with cervical dystonia by bilateral deep brain stimulation: a case series report. Clin. Neurol. Neurosurg. 190, 105644. https://doi.org/10.1016/j.clineuro.2019.105644.

Fasano, A., Llinas, M., Munhoz, R.P., Hlasny, E., Kucharczyk, W., Lozano, A.M., 2017. MRI-guided focused ultrasound thalamotomy in non-ET tremor syndromes. Neurology. 89 (8), 771–775. https://doi.org/10.1212/WNL.0000000000004268.

Tsuboi, T., Wong, J.K., Eisinger, R.S., et al. 2021. Comparative connectivity correlates of dystonic and essential tremor deep brain stimulation. *Brain*. doi:10.1093/brain/awab074.

DeSimone, J.C., Archer, D.B., Vaillancourt, D.E., Wagle Shukla, A. 2019. Network-level connectivity is a critical feature distinguishing dystonic tremor and essential tremor. *Brain* doi:10.1093/brain/awz085.

Broersma, M., van der Stouwe, A.M.M., Buijink, A.W.G., de Jong, B.M., Groot, P.F.C., Speelman, J.D., Tijssen, M.A.J., van Rootselaar, A.-F., Maurits, N.M., 2016. Bilateral cerebellar activation in unilaterally challenged essential tremor. Neuroimage Clin. 11, 1–9. https://doi.org/10.1016/j.nicl.2015.12.011.

Buijink, A.W.G., van der Stouwe, A.M.M., Broersma, M., Sharifi, S., Groot, P.F.C., Speelman, J.D., Maurits, N.M., van Rootselaar, A.-F., 2015. Motor network disruption in essential tremor: a functional and effective connectivity study. Brain 138 (10), 2934–2947. https://doi.org/10.1093/brain/awv225.

Pan, M.-K., Li, Y.-S., Wong, S.-B., Ni, C.-L., Wang, Y.-M., Liu, W.-C., Lu, L.-Y., Lee, J.-C., Cortes, E.P., Vonsattel, J.-P., Sun, Q., Louis, E.D., Faust, P.L., Kuo, S.-H., 2020. Cerebellar oscillations driven by synaptic pruning deficits of cerebellar climbing fibers contribute to tremor pathophysiology. Sci. Transl. Med. 12 (526) https://doi.org/10.1126/scitranslmed.aay1769.

Gallea, C., Popa, T., García-Lorenzo, D., Valabregue, R., Legrand, A.-P., Marais, L., Degos, B., Hubsch, C., Fernández-Vidal, S., Bardinet, E., Roze, E., Lehéricy, S., Vidailhet, M., Meunier, S., 2015. Intrinsic signature of essential tremor in the cerebello-frontal network. Brain. 138 (10), 2920–2933. https://doi.org/10.1093/brain/awv171.

Kirke, D.N., Battistella, G., Kumar, V., Rubien-Thomas, E., Choy, M., Rumbach, A., Simonyan, K., 2017. Neural correlates of dystonic tremor: a multimodal study of voice tremor in spasmodic dysphonia. Brain Imaging Behav. 11 (1), 166–175. https://doi.org/10.1007/s11682-016-9513-x.

Battistella, G., Simonyan, K., 2019. Top-down alteration of functional connectivity within the sensorimotor network in focal dystonia. Neurology 92 (16), E1843–E1851. https://doi.org/10.1212/Wnl.0000000000007317.

Cerasa, A., Nisticò, R., Salsone, M., Bono, F., Salvino, D., Morelli, M., Arabia, G., Quattrone, A., 2014. Neuroanatomical correlates of dystonic tremor: a cross-sectional study. Parkinsonism Related Disord. 20 (3), 314–317. https://doi.org/10.1016/j.parkreldis.2013.12.007.

Antelmi, E., Di Stasio, F., Rocchi, L., Erro, R., Liguori, R., Ganos, C., Brugger, F., Teo, J., Berardelli, A., Rothwell, J., Bhatia, K.P., 2016. Impaired eye blink classical conditioning distinguishes dystonic patients with and without tremor. Parkinsonism Relat Disord. 31, 23–27. https://doi.org/10.1016/j.parkreldis.2016.06.011.

Conte, A., Ferrazzano, G., Belvisi, D., Manzo, N., Battista, E., Li Voti, P., Nardella, A., Fabbrini, G., Berardelli, A., 2018. Somatosensory temporal discrimination in Parkinson's disease, dystonia and essential tremor: pathophysiological and clinical implications. Clin. Neurophysiol. 129 (9), 1849–1853. https://doi.org/10.1016/j.clinph.2018.05.024.

Helmich, R.C., Janssen, M.J.R., Oyen, W.J.G., Bloem, B.R., Toni, I. 2011. Pallidal dysfunction drives a cerebellothalamic circuit into Parkinson tremor. *Ann. Neurol.* 69 (2), 269-281. doi:10.1002/ana.22361.

Dirkx, M.F., Zach, H., van Nuland, A.J., Bloem, B.R., Toni, I., Helmich, R.C., 2020. Cognitive load amplifies Parkinson's tremor through excitatory network influences onto the thalamus. Brain 143 (5), 1498–1511. https://doi.org/10.1093/brain/awaa083.

Nieuwhof, F., Bie, R.M.A., Praamstra, P., Munckhof, P., Helmich, R.C., 2020. The cerebral tremor circuit in a patient with Holmes tremor. Ann. Clin. Transl. Neurol. 7 (8), 1453–1458.

Nuland, A.J.M., Ouden, H.E.M., Zach, H., Dirkx, M.F.M., Asten, J.J.A., Scheenen, T.W.J., Toni, I., Cools, R., Helmich, R.C., 2020. GABAergic changes in the thalamocortical circuit in Parkinson's disease. Hum. Brain Mapp. 41 (4), 1017–1029. https://doi.org/10.1002/hbm.24857.

Lustenhouwer, R., van Alfen, N., Cameron, I.G.M., Toni, I., Geurts, A.C.H., Helmich, R.C., van Engelen, B.G.M., Groothuis, J.T., 2019. NA-CONTROL: a study protocol for a randomised controlled trial to compare specific outpatient rehabilitation that targets cerebral mechanisms through relearning motor control and uses self-management strategies to improve functional capability of the upper extremity, to usual care in patients with neuralgic amyotrophy. Trials 20 (1). https://doi.org/10.1186/s13063-019-3556-4.

Pandey, S., Bhattad, S., Hallett, M. 2020. The problem of questionable dystonia in the diagnosis of 'essential tremor-plus'. *Tremor Other Hyperkinet Mov (N Y)*. 10, 27. doi: 10.5334/tohm.539.

Dirkx, M.F., den Ouden, H., Aarts, E., Timmer, M., Bloem, B.R., Toni, I., Helmich, R.C., 2016. The cerebral network of Parkinson's tremor: an effective connectivity fMRI study. J. Neurosci. 36 (19), 5362–5372.

Pruim, R.H., Mennes, M., Buitelaar, J.K., Beckmann, C.F., 2015. Evaluation of ICA-AROMA and alternative strategies for motion artifact removal in resting state fMRI. Neuroimage 112, 278–287. https://doi.org/10.1016/j.neuroimage.2015.02.063.

Pruim, R.H., Mennes, M., van Rooij, D., Llera, A., Buitelaar, J.K., Beckmann, C.F., 2015. ICA-AROMA: a robust ICA-based strategy for removing motion artifacts from fMRI data. Neuroimage 112, 267–277. https://doi.org/10.1016/j.neuroimage.2015.02.064.

Diedrichsen, J., 2006. A spatially unbiased atlas template of the human cerebellum. Neuroimage 33 (1), 127–138. https://doi.org/10.1016/j.neuroimage.2006.05.056.

Lund, T.E., Norgaard, M.D., Rostrup, E., Rowe, J.B., Paulson, O.B., 2005. Motion or activity: their role in intra- and inter-subject variation in fMRI. Neuroimage 26 (3), 960–964. https://doi.org/10.1016/j.neuroimage.2005.02.021.

Friston, K.J., Harrison, L., Penny, W., 2003. Dynamic causal modelling. Neuroimage 19 (4), 1273–1302. https://doi.org/10.1016/s1053-8119(03)00202-7.

Buckner, R.L., Krienen, F.M., Castellanos, A., Diaz, J.C., Yeo, B.T., 2011. The organization of the human cerebellum estimated by intrinsic functional connectivity. J. Neurophysiol. 106 (5), 2322–2345. https://doi.org/10.1152/jn.00339.2011.

Dirkx, M.F., den Ouden, H.E., Aarts, E., et al. 2017. Dopamine controls Parkinson's tremor by inhibiting the cerebellar thalamus. *Brain* 140(3), 721-734. doi:10.1093/brain/aww331.

Penny, W.D., Stephan, K.E., Daunizeau, J., et al. 2010. Comparing families of dynamic causal models. *PLoS Comput. Biol.* 6(3), e1000709. doi:10.1371/journal.pcbi.1000709.

Stephan, K.E., Penny, W.D., Moran, R.J., den Ouden, H.E., Daunizeau, J., Friston, K.J., 2010. Ten simple rules for dynamic causal modeling. Neuroimage 49 (4), 3099–3109. https://doi.org/10.1016/j.neuroimage.2009.11.015.

Ly, A., Verhagen, J., Wagenmakers, E.J., 2016. Harold Jeffreys's default Bayes factor hypothesis tests: explanation, extension, and application in psychology. J. Math. Psychol. 72, 19–32. https://doi.org/10.1016/j.jmp.2015.06.004.

Ly, A., Marsman, M., Wagenmakers, E.-J., 2018. Analytic posteriors for Pearson's correlation coefficient. Stat. Neerl. 72 (1), 4–13. https://doi.org/10.1111/stan.12111.

Ashburner, J., 2007. A fast diffeomorphic image registration algorithm. Neuroimage 38 (1), 95–113. https://doi.org/10.1016/j.neuroimage.2007.07.007.

Prodoehl, J., Yu, H., Little, D.M., Abraham, I., Vaillancourt, D.E., 2008. Region of interest template for the human basal ganglia: comparing EPI and standardized space approaches. Neuroimage 39 (3), 956–965. https://doi.org/10.1016/j.neuroimage.2007.09.027.

Maldjian, J.A., Laurienti, P.J., Kraft, R.A., Burdette, J.H., 2003. An automated method for neuroanatomic and cytoarchitectonic atlas-based interrogation of fMRI data sets. Neuroimage 19 (3), 1233–1239. https://doi.org/10.1016/s1053-8119(03)00169-1.

Maldjian, J.A., Laurienti, P.J., Burdette, J.H., 2004. Precentral gyrus discrepancy in electronic versions of the Talairach atlas. Neuroimage 21 (1), 450–455. https://doi.org/10.1016/j.neuroimage.2003.09.032.

Niemann, K., Mennicken, V.R., Jeanmonod, D., Morel, A., 2000. The morel stereotactic atlas of the human thalamus: atlas-to-MR registration of internally consistent canonical model. Neuroimage. 12 (6), 601–616. https://doi.org/10.1006/nimg.2000.0650.

Mai, J.K., Majtanik, M., 2018. Toward a common terminology for the thalamus. Front. Neuroanat. 12, 114. https://doi.org/10.3389/fnana.2018.00114.

Hirai, T., Jones, E.G., 1989. A new parcellation of the human thalamus on the basis of histochemical staining. *Brain Res. Rev.* 14 (1), 1–34. https://doi.org/10.1016/0165-0173(89)90007-6.

Krack, P., Pollak, P., Limousin, P., Benazzouz, A., Benabid, A.L., 1997. Stimulation of subthalamic nucleus alleviates tremor in Parkinson's disease. Lancet 350 (9092), 1675. https://doi.org/10.1016/S0140-6736(97)24049-3.

Hutchison, W.D., Lozano, A.M., Tasker, R.R., Lang, A.E., Dostrovsky, J.O., 1997. Identification and characterization of neurons with tremor-frequency activity in human globus pallidus. Exp. Brain Res. 113 (3), 557–563. https://doi.org/10.1007/pl00005606.

Percheron, G., Francois, C., Talbi, B., Yelnik, J., Fenelon, G., 1996. The primate motor thalamus. Brain Res. Rev. 22 (2), 93–181.

Helmich, R.C., Hallett, M., Deuschl, G., Toni, I., Bloem, B.R. 2012. Cerebral causes and consequences of parkinsonian resting tremor: a tale of two circuits? *Brain* 135(11), 3206-3226. doi:10.1093/brain/aws023.

Smith, S.M., Nichols, T.E., 2009. Threshold-free cluster enhancement: addressing problems of smoothing, threshold dependence and localisation in cluster inference. Neuroimage 44 (1), 83–98. https://doi.org/10.1016/j.neuroimage.2008.03.061.

Eickhoff, S.B., Stephan, K.E., Mohlberg, H., Grefkes, C., Fink, G.R., Amunts, K., Zilles, K., 2005. A new SPM toolbox for combining probabilistic cytoarchitectonic maps and functional imaging data. Neuroimage 25 (4), 1325–1335. https://doi.org/10.1016/j.neuroimage.2004.12.034.

Brett, M., Anton, J., Valabregue, R., Poline, J. 2002. Region of interest analysis using an SPM toolbox. *[abstract] Presented at the 8th International Conference on Functional Mapping of the Human Brain, June 2-6, 2002, Sendai, Japan Available on CD-ROM in NeuroImage, 16(2)*.

Deuschl, G., Wilms, H., Krack, P., Wurker, M., Heiss, W.D., 1999. Function of the cerebellum in Parkinsonian rest tremor and Holmes' tremor. Ann. Neurol. 46 (1), 126–128. https://doi.org/10.1002/1531-8249(199907)46:1<126::aid-ana20>3.0.co;2-3.

Rouder, J.N., Morey, R.D., Speckman, P.L., Province, J.M., 2012. Default Bayes factors for ANOVA designs. J. Math. Psychol. 56 (5), 356–374. https://doi.org/10.1016/j.jmp.2012.08.001.

Wagenmakers, E.-J., Love, J., Marsman, M., Jamil, T., Ly, A., Verhagen, J., Selker, R., Gronau, Q.F., Dropmann, D., Boutin, B., Meerhoff, F., Knight, P., Raj, A., van Kesteren, E.-J., van Doorn, J., Šmíra, M., Epskamp, S., Etz, A., Matzke, D., de Jong, T., van den Bergh, D., Sarafoglou, A., Steingroever, H., Derks, K., Rouder, J.N., Morey, R.D., 2018. Bayesian inference for psychology. Part II: example applications with JASP. Psychon. Bull. Rev. 25 (1), 58–76. https://doi.org/10.3758/s13423-017-1323-7.

Stacy, M.A., Elble, R.J., Ondo, W.G., Wu, S.C., Hulihan, J., group TRSs., 2007. Assessment of interrater and intrarater reliability of the Fahn-Tolosa-Marin Tremor Rating Scale in essential tremor. Mov. Disord. 22 (6), 833–838. https://doi.org/10.1002/mds.21412.

Burke, R.E., Fahn, S., Marsden, C.D., Bressman, S.B., Moskowitz, C., Friedman, J., 1985. Validity and reliability of a rating scale for the primary torsion dystonias. Neurology 35 (1), 73–77.

Hoops, S., Nazem, S., Siderowf, A.D., Duda, J.E., Xie, S.X., Stern, M.B., Weintraub, D., 2009. Validity of the MoCA and MMSE in the detection of MCI and dementia in Parkinson disease. Neurology 73 (21), 1738–1745. https://doi.org/10.1212/WNL.0b013e3181c34b47.

Nasreddine, Z.S., Phillips, N.A., BÃ©dirian, V., Charbonneau, S., Whitehead, V., Collin, I., Cummings, J.L., Chertkow, H., 2005. The montreal cognitive assessment, MoCA: a brief screening tool for mild cognitive impairment. J. Am. Geriatr. Soc. 53 (4), 695–699. https://doi.org/10.1111/j.1532-5415.2005.53221.x.

Dubois, B., Slachevsky, A., Litvan, I., Pillon, B., 2000. The FAB - A frontal assessment battery at bedside. Neurology 55 (11), 1621–1626.

van Loo, E.H., Wiebrands, C., van Laar, T., 2007. De 'Frontal Assessment Battery' (FAB) voor screening op frontaalkwabpathologie bij neurodegeneratieve ziekten. Tijdschr Neurol Neurochir. 108, 115–120.

Martino, D., Bonassi, G., Lagravinese, G., Pelosin, E., Abbruzzese, G., Avanzino, L., 2020. Defective human motion perception in cervical dystonia correlates with coexisting tremor. Mov. Disord. 35 (6), 1067–1071. https://doi.org/10.1002/mds.28017.

White, J.J., Sillitoe, R.V., 2017. Genetic silencing of olivocerebellar synapses causes dystonia-like behaviour in mice. Nat. Commun. 8 (1) https://doi.org/10.1038/ncomms14912.

Latorre, A., Rocchi, L., Bhatia, K.P., 2020. Delineating the electrophysiological signature of dystonia. Exp. Brain Res. 238 (7-8), 1685–1692.

Hallett, M., de Haan, W., Deco, G., Dengler, R., Di Iorio, R., Gallea, C., Gerloff, C., Grefkes, C., Helmich, R.C., Kringelbach, M.L., Miraglia, F., Rektor, I., Strýček, O., Vecchio, F., Volz, L.J., Wu, T., Rossini, P.M., 2020. Human brain connectivity: clinical applications for clinical neurophysiology. Clin. Neurophysiol. 131 (7), 1621–1651. https://doi.org/10.1016/j.clinph.2020.03.031.

Gallea, C., Herath, P., Voon, V., Lerner, A., Ostuni, J., Saad, Z., Thada, S., Solomon, J., Horovitz, S.G., Hallett, M., 2018. Loss of inhibition in sensorimotor networks in focal hand dystonia. Neuroimage Clin. 17, 90–97. https://doi.org/10.1016/j.nicl.2017.10.011.

Maas, R.P.P.W.M., Helmich, R.C.G., Warrenburg, B.P.C., 2020. The role of the cerebellum in degenerative ataxias and essential tremor: Insights from noninvasive modulation of cerebellar activity. Mov. Disord. 35 (2), 215–227. https://doi.org/10.1002/mds.27919.

Delnooz, C.C., Helmich, R.C., Medendorp, W.P., Van de Warrenburg, B.P., Toni, I., Mar 2013. Writer's cramp: increased dorsal premotor activity during intended writing. Hum. Brain Mapp. 34 (3), 613–625. https://doi.org/10.1002/hbm.21464.

Coenen, V.A., Sajonz, B., Prokop, T., Reisert, M., Piroth, T., Urbach, H., Jenkner, C., Reinacher, P.C., 2020. The dentato-rubro-thalamic tract as the potential common deep brain stimulation target for tremor of various origin: an observational case series. Acta Neurochir (Wien) 162 (5), 1053–1066. https://doi.org/10.1007/s00701-020-04248-2.

Panyakaew, P., Cho, H.J., Lee, S.W., Wu, T., Hallett, M., 2020. The pathophysiology of dystonic tremors and comparison with essential tremor. J. Neurosci. 40 (48), 9317–9326. https://doi.org/10.1523/jneurosci.1181-20.2020.

Dirkx, M.F., Zach, H., van Nuland, A., Bloem, B.R., Toni, I., Helmich, R.C., 2019. Cerebral differences between dopamine-resistant and dopamine-responsive Parkinson's tremor. Brain 142 (10), 3144–3157. https://doi.org/10.1093/brain/awz261.

Coenen, V.A., Allert, N., Paus, S., Kronenburger, M., Urbach, H., Madler, B. 2014. Modulation of the cerebello-thalamo-cortical network in thalamic deep brain stimulation for tremor: a diffusion tensor imaging study. *Neurosurgery* 75(6), 657-669; discussion 669-70. doi:10.1227/NEU.0000000000000540.

Milosevic, L., Kalia, S.K., Hodaie, M., Lozano, A.M., Popovic, M.R., Hutchison, W.D., 2018. Physiological mechanisms of thalamic ventral intermediate nucleus stimulation for tremor suppression. *Brain* 141 (7), 2142–2155. https://doi.org/10.1093/brain/awy139.

Kassubek, J., Juengling, F.D., Hellwig, B., Spreer, J., Lucking, C.H. 2002. Thalamic gray matter changes in unilateral Parkinsonian resting tremor: a voxel-based morphometric analysis of 3-dimensional magnetic resonance imaging. *Neurosci. Lett.* 323(1), 29-32. doi:Pii S0304-3940(02)00111-8 Doi 10.1016/S0304-3940(02)00111-8.

Maguire, E.A., Gadian, D.G., Johnsrude, I.S., Good, C.D., Ashburner, J., Frackowiak, R.S.J., Frith, C.D., 2000. Navigation-related structural change in the hippocampi of taxi drivers. Proc. Natl. Acad. Sci. USA 97 (8), 4398–4403. https://doi.org/10.1073/pnas.070039597.

Bostan, A.C., Strick, P.L., 2018. The basal ganglia and the cerebellum: nodes in an integrated network. Nat. Rev. Neurosci. 19 (6), 338–350. https://doi.org/10.1038/s41583-018-0002-7.

Filip, P., Gallea, C., Lehericy, S., et al., 2017. Disruption in cerebellar and basal ganglia networks during a visuospatial task in cervical dystonia. Mov. Disord. 32 (5), 757–768. https://doi.org/10.1002/mds.26930.

Bostan, A.C., Dum, R.P., Strick, P.L., 2010. The basal ganglia communicate with the cerebellum. Proc. Natl. Acad. Sci. USA 107 (18), 8452–8456. https://doi.org/10.1073/pnas.1000496107.

Hoshi, E., Tremblay, L., Feger, J., Carras, P.L., Strick, P.L., 2005. The cerebellum communicates with the basal ganglia. Nat. Neurosci. 8 (11), 1491–1493. https://doi.org/10.1038/nn1544.

Sedov, A., Usova, S., Semenova, U., Gamaleya, A., Tomskiy, A., Beylergil, S.B., Jinnah, H. A., Shaikh, A.G., 2020. Pallidal activity in cervical dystonia with and without head tremor. Cerebellum 19 (3), 409–418.

Maurer, C.W., LaFaver, K., Ameli, R., Epstein, S.A., Hallett, M., Horovitz, S.G. 2016. Impaired self-agency in functional movement disorders. *A resting-state fMRI study*. 87 (6), 564-570. doi:10.1212/wnl.0000000000002940.